

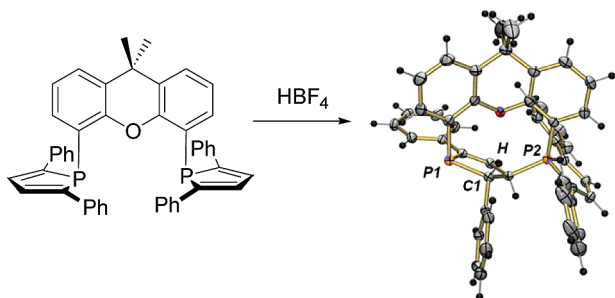
**Protonation of a Xantphos–Phosphole Ligand.
Intramolecular Trapping of a P–H Phospholium Salt**

Aurélie Escalle, Xavier F. Le Goff, and Pascal Le Floch*

Laboratoire “Hétéroéléments et Coordination”, Ecole Polytechnique, CNRS, 91128 Palaiseau Cedex, France

pascal.lefloch@polytechnique.edu

Received July 10, 2009



Protonation of a bidentate xantphos–phosphole ligand by HBF_4 affords only one enantiomer of a cyclic phospholium dihydropholene structure. DFT calculations allowed us to establish that protonation initially takes place at the phosphorus atom of the phosphole moiety to afford a transient P–H phospholium salt, which in turn protonates the $\text{C}=\text{C}$ double bond of the second phosphole unit.

Due to the presence of both a reactive phosphorus lone pair and a dienic system, phospholes exhibit a reactivity that markedly differs from that of classical phosphines bearing unsaturated substituents. In most cases, reactivity at phosphorus and at the dienic system is linked, and not surprisingly, coordination of the phosphorus lone pair was shown to dramatically influence the reactivity of the unsaturated π -system. Thus, transition metal complexes as well as phosphole oxide and sulfide were extensively used to prepare new phosphorus heterocycles,¹ reactive intermediates,² and precursors of molecular materials.³

Comparatively, little attention has been paid to phospholium salts, the phosphole equivalents of phosphoniums,

which have found numerous applications in organic synthesis (Wittig reaction), and quaternarization of the phosphorus lone pair has been considerably less exploited to modulate the reactivity of the phosphole nucleus. Thus, though some phospholium salts have been identified,⁴ protonated phospholes eluded isolation so far and their chemistry remains unexplored.⁵ Theoretical calculations suggest that this situation mainly results from the presence of two potential protonation sites at the phosphole nucleus, the phosphorus lone pair and the two α -carbon atoms (C2 and C5 positions).⁶ Thus, protonation may occur either at phosphorus or on the dienic system depending on the substitution scheme of the ring to yield rather unstable species. In the course of our studies on 2,5-diphenylphosphole derivatives,⁷ we recently investigated this protonation process in the case of a xantphos derivative and found that this chelate backbone allowed us to put in evidence an intramolecular trapping reaction of a P–H phospholium salt. Herein we wish to report on these results.

Reaction of XDPP **1** (XDPP is xantphos-2,5-diphenylphosphole) with 1.5 equiv of HBF_4 (54 wt % in Et_2O) at room temperature resulted in an exothermic reaction and the immediate formation of a new compound **2**, which was evidenced in ^{31}P NMR spectroscopy by a AB spin system pattern. Compound **2-S**, which proved to be remarkably air- and water-stable, was isolated after usual workup as a yellow crystalline compound in nearly quantitative yield. Formulation of **2-S** (*S* corresponding to the stereochemistry of the C_α -protonated site) could not be straightforwardly assessed on the exclusive basis of ^1H and ^{13}C NMR data, and an X-ray crystal structure determination proved to be very useful. As can be seen in Figure 1, **2-S** is a cyclic structure featuring a 2,3-dihydrophospholene unit connected to the phosphorus atom of a phospholium unit through the C_α carbon atom (Scheme 1).

Importantly, only one diastereomer is formed, and no trace of the **2-R** derivative was detected in the reaction mixture. This type of structure is not totally unprecedented, and in 1986, during a study on the protonation of the 1-*P*-phenyl-3,4-dimethylphosphole, Quin and Mathey evidenced

(4) See ref 1b; p 219.

(5) (a) Chuchman, R.; Holah, D. G.; Hughes, A. N.; Hui, B. C. *J. Heterocycl. Chem.* **1971**, *8*, 877. (b) Quin, L. D.; Mesch, K. A.; Orton, W. L. *Phosphorus Sulfur* **1982**, *12*, 161.

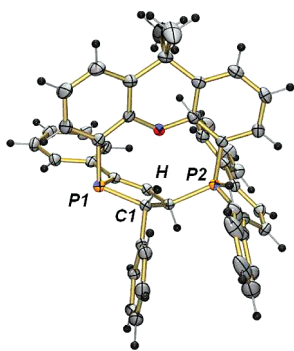
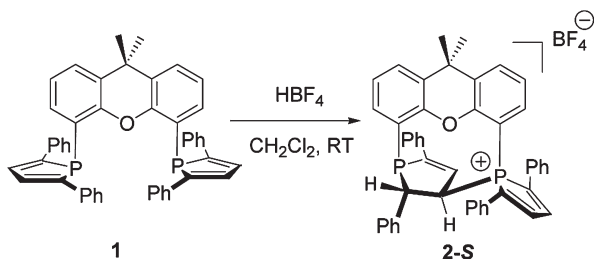
(6) (a) Delaere, D.; Pham-Tran, N.; Nguyen, M. T. *J. Phys. Chem. A* **2003**, *107*, 7514. (b) Delaere, D.; Pham-Tran, N.; Nguyen, M. T. *Chem. Phys. Lett.* **2004**, *383*, 138.

(7) (a) Thoumazet, C.; Melaimi, M.; Ricard, L.; Mathey, F.; Le Floch, P. *Organometallics* **2003**, *22*, 1580. (b) Melaimi, M.; Thoumazet, C.; Ricard, L.; Le Floch, P. *J. Organomet. Chem.* **2004**, *689*, 2988. (c) Thoumazet, C.; Melaimi, M.; Ricard, L.; Le Floch, P. *C.R. Chimie* **2004**, *8–9*, 823. (d) Thoumazet, C.; Ricard, L.; Grutzmacher, H.; Le Floch, P. *Chem. Commun.* **2005**, 1592. (e) Thoumazet, C.; Ricard, L.; Grutzmacher, H.; Le Floch, P. *Eur. J. Inorg. Chem.* **2006**, *19*, 3911. (f) Mora, G.; van Zutphen, S.; Thoumazet, C.; Le Goff, X.-F.; Ricard, L.; Grutzmacher, H.; Le Floch, P. *Organometallics* **2005**, *25*, 5528. (g) Mora, G.; Piechaczyk, O.; Le Goff, X.-F.; Le Floch, P. *Organometallics* **2008**, *27*, 2565. (h) Mora, G.; Deschamps, B.; van Zutphen, S.; Le Goff, X.-F.; Ricard, L.; Le Floch, P. *Organometallics* **2007**, *26*, 1846. (i) Mora, G.; van Zutphen, S.; Klemp, C.; Ricard, L.; Le Goff, X.-F.; Jean, Y.; Le Floch, P. *Inorg. Chem.* **2007**, *46*, 10365. (j) Mora, G.; Piechaczyk, O.; Houdard, R.; Mézailles, N.; Le Goff, X.-F.; Le Floch, P. *Chem.—Eur. J.* **2008**, *14*, 10047.

(1) (a) Mathey, F. Phospholes. In *Science of Synthesis*; Maas, G., Ed.; Thieme: Stuttgart, Germany, 2001; p 553. (b) Quin, L. D. *Phosphorus–Carbon Heterocyclic Chemistry: The Rise of a New Domain*; Mathey, F., Ed.; Pergamon: Amsterdam, 2001; p 219.

(2) (a) Mathey, F. *Chem. Rev.* **1988**, *88*, 429. (b) Mathey, F. *Angew. Chem., Int. Ed.* **2003**, *42*, 1578. (c) Dillon, K.; Mathey, F.; Nixon, J. F. *Phosphorus: The Carbon Copy*; John Wiley and Sons: Chichester, UK, 1998.

(3) (a) Baumgartner, T.; Réau, R. *Chem. Rev.* **2006**, *106*, 4681. (b) Crassoux, J.; Réau, R. *Dalton Trans.* **2008**, 6865. (c) Hissler, M.; Lescop, C.; Réau, R. *Pure Appl. Chem.* **2007**, *79*, 201.

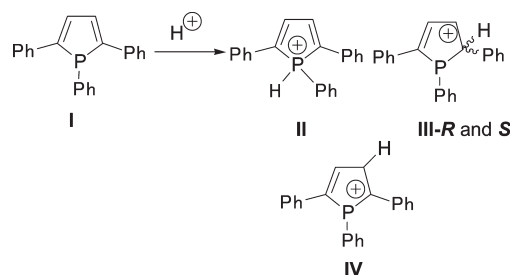
FIGURE 1. ORTEP view of one molecule of **2-S**.SCHEME 1. Synthesis of **2**

the transient formation of a similar dimer obtained by deprotonation of a dimeric diphospholium salt. However, this compound was found too sensitive to be fully characterized.⁸ Formation of **2-S** raises an interesting mechanistic problem, and three distinct mechanisms can be proposed. First, one may propose that protonation initially takes place at the C_{α} carbon atom of one phosphole ring (P1) to transiently afford a 2,3-dihydrophospholenium ion, which in turn reacts with the phosphorus atom of the second phosphole unit (P2) through its C_{β} carbon atom to afford **2-S**. However, this mechanism seems unlikely since it would suppose that protonation regioselectively would take place at the C_{α} carbon atom to exclusively afford a single diastereomer. The second possible mechanism involves, in a first step, the protonation of one phosphole ring (P2) to afford a P–H phospholium derivative, which would subsequently react through its P–H bond to give a concerted addition onto the C=C double bond of the second phosphole moiety. Finally, the third mechanism, which also relies on the transient formation of a P–H phospholium salt, would involve the transfer of the proton from phosphorus to the C_{α} carbon atom followed by the attack of the phosphorus atom onto the cationic C_{β} carbon atom of the 2,3-dihydrophospholenium formed. In order to shed some light on the second and third proposals, DFT calculations were carried out.

We first put our attention on the preferred protonation site of the XDPP ligand. Assuming that the xantphos backbone could be modeled by a simple phenyl group, calculations were carried out on the 1,2,5-triphenylphosphole (TPP) derivative **I**. Calculations of the proton affinity of phosphole derivatives in the gas phase and in solution have already been the subject of some investigations, and it has been shown that

TABLE 1. Proton Affinity of **I** Computed with Methods 1 and 2 (PAs are given in kcal/mol)

compound	method 1	method 2
II	–220.64	–221.97
III-R	–219.67	–220.07
III-S	–215.72	–216.22
IV	–210.12	–213.41

SCHEME 2. Protonation of TPP **I**

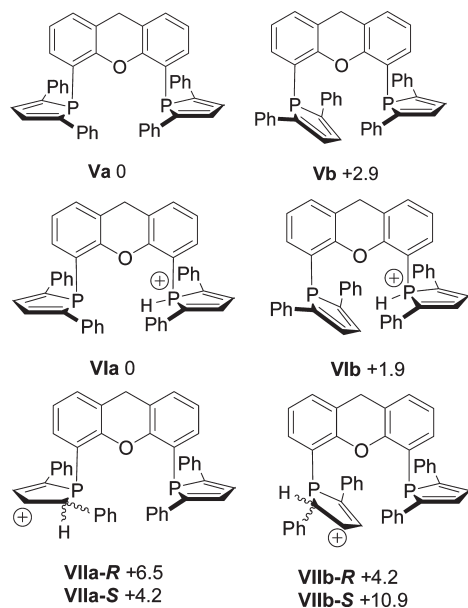
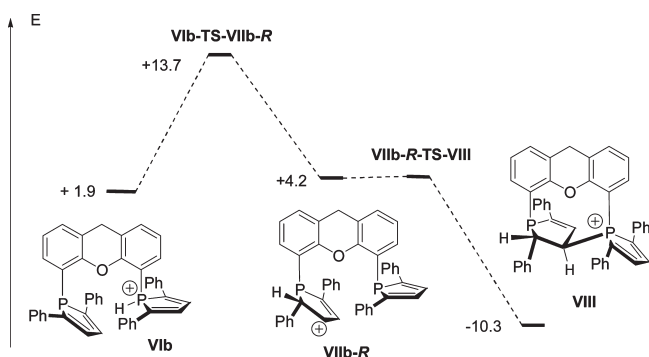
the favored protonation site is highly sensitive to the substitution scheme of the phosphole unit. The proton affinity of **I** was computed using the method developed by Nguyen et al. at the B3LYP/6-311++G(d,p)//HF/6-31G(d,p) (method 1) level and by a second method at the B3PW91/6-311++G(d,p)//B3PW91/6-311 G(d,p) (method 2) level of theory. Results of these calculations, which are summarized in Table 1, led to the same conclusion and indicate that the phosphorus atom is the favored protonation site (Scheme 2).

Having established that a P–H phospholium salt is probably formed in a first step upon protonation, we then turned our attention to the conformation of the XDPP ligand. Calculations suggest that, at room temperature, two conformations exist and can interconvert. Two motions can explain the interconversion between these two conformers: a rotation around the P–C that connects the phosphole unit to the xantphos backbone and the inversion of the phosphorus atom. The first motion can be excluded due to the bulkiness provided by the ancillary phenyl groups. The inversion of the phosphorus atom is therefore the most realistic motion. Indeed, the inversion barrier of the TPP ligand was found to be rather low at 16.0 kcal/mol, and we can assume that this also stands for **I** if we consider that the xantphos backbone can be modeled by a phenyl group. Both conformers of XDPP, **Va** and **Vb**, were found to be very close in energy (Scheme 3). All possible C_{α} - and P-protonated derivatives were optimized, and their relative energies were compared with regards to **Va** (Scheme 3).⁹ Both conformers of **V** (**a** and **b**) are very close in energy as well as their respective H–P phospholium salts **VIa** and **b**. It also appears that, in good agreement with calculations of the TPP **I**, the C_{α} -protonated compounds **VIIa** and **VIIb** lie at an energy (+4.2 kcal/mol) higher than that of **VIa** and **VIb**.

On the basis of these results, we then focused our study on the determination of the complete pathway rationalizing the formation of **2**. The overall computed energetic pathway is presented in Scheme 4, with the energies being related to compound **VIa**. Various attempts were made to characterize

(8) Quin, L. D.; Belmont, S. E.; Mathey, F.; Charrier, C. *J. Chem. Soc., Perkin Trans. 2* **1986**, 629.

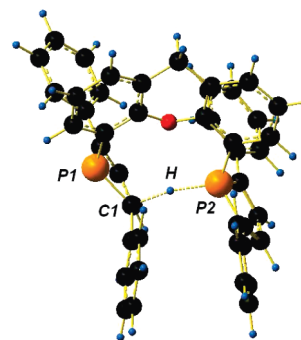
(9) The theoretical structure of the O-protonated derivative of **V** was also successfully optimized but was found very high in energy at +27.6 kcal/mol.

SCHEME 3. Relative Energies (in kcal/mol) of **V** and Their Related Protonated Derivatives **VI** and **VII**SCHEME 4. Calculated Energetic Pathway Summarizing the Transformation of **VIb** into **VIII**

a transition step connecting **VIb** to **VIII**. However, these calculations did not allow us to conclude that a concerted addition of the P–H bond onto the C=C bond of the second phosphole moiety takes place.

A mechanism involving two distinct steps was found (third proposal). As expected, the first step involves a transfer of the proton from the phosphorus atom of the P–H phospholium moiety of **VIb** to the C α carbon atom of the second phosphole moiety to afford the 2,3-dihydrophospholenium intermediate **VIIb-R**, which was characterized as a minimum on the PES. As can be seen, this proton transfer requires weak activation energy and is therefore compatible with the experimental conditions employed.

A view of the computed structure of **VIb-TS-VIIb-R** is presented in Figure 2. As expected when considering respective energies, the structure of **VIb-TS-VIIb-R** lies between that of the **VIb** and **VIIb-R** and the proton is located at 1.725 Å of the P2 atom and 1.461 Å of C1. In terms of MOs, this reaction involves the interaction of H⁺ with the π_2 orbital (mainly developed on C α carbon atoms) of the butadienyl moiety of the phosphole unit (see Supporting Information).

FIGURE 2. View of the computed structure of **VIb-TS-VIIb-R**.

The second step leading to **VIII** involves the reaction of the phosphorus atom lone pair on the C β carbon atom of the 2,3-dihydrophospholenium unit. The transition state of this second step lies at the same energy as that of **VIIb-R** (no significant energy difference) and corresponds to a motion of the dihydrophospholenium unit toward the P2 atom.¹⁰

In conclusion, we have shown that the protonation of the XDPP ligand involves two distinct protonation steps, the first one occurring at phosphorus according to the slightly greater proton affinity of phosphorus. However, this weak energetic difference accounts for the results observed with the 1,2,5-triphenylphosphole. Protonation under the same conditions leads to the formation of unidentified compounds, and one may therefore propose that, though the formation of the P–H phospholium is favored, both phospholium species (P- and C α -protonated) are probably present in solution since the P–H phospholium salt can act as a proton source.¹¹

Experimental Section

Synthesis of 2. To a solution of XDPP **1** (100 mg, 0.15 mmol) in dichloromethane was added 1.5 equiv of HBF₄ (54 wt % in diethylether) (25.7 μ L, 0.22 mmol). The color of the solution changed to a very deep yellow, and the reaction was found to be strongly exothermic. After 5 min, the completion of the reaction was checked by ³¹P NMR. Solvents were evaporated, and the solid was washed with diethylether. Compound **2-S** was obtained as a yellow solid with 96% yield (109 mg): ³¹P{¹H} NMR (CH₂Cl₂, 121.5 MHz) δ 30.3 (s), 36.7 (s); ¹H NMR (CD₃CN, 300 MHz) δ 1.49 (s, 3H, CH₃), 1.94 (s, 3H, CH₃), 4.51 (ddd, ²J_{HP} = 24.3 Hz, ³J_{HP} = 5.2 Hz, ³J_{HH} = 2.9 Hz, 1H, H α P), 4.82 (ddt, ²J_{HP} = 16.6 Hz, ³J_{HP} = 7.8 Hz, ³J_{HH} = 3.1 Hz, 1H, H α P₊), 6.20 (ddd, ³J_{HP} = 9.1 Hz, ³J_{HP} = 4.2 Hz, ³J_{HH} = 3.2 Hz, 1H, H β -protonated phosphole), 6.66 (m, 2H, H_{aromatic}), 7.00–8.10 (m, 26H, H_{aromatic} and H β -phosphole); ¹³C NMR (CD₃CN, 75.5 MHz) δ 26.9 (s, CH₃), 34.0 (s, CH₃), 37.4 (s, C, C(CH₃)₂), 45.8 (dd, J = 14.6 Hz, J = 5.9 Hz, CH, CH α -protonated bond phosphole), 57.8 (dd,

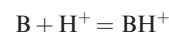
(10) **VIIb-R-TS-VIII** features one imaginary frequency at -20.53 cm⁻¹. Single-point calculations indicate that, at the B3PW91/6-31+G* level of theory, this TS lies above **VIIb-R** (ΔE_{ZPE} = +0.1 kcal/mol) but not at the B3PW91/6-311++G** (ΔE_{ZPE} = -1.2 kcal/mol). Taking into account the exothermicity of the transformation, one may propose that the structure of this transition state is very close to that of **VIIb-R** and that no significant activation barrier is needed to promote the attack of the P atom lone pair onto the cationic carbon atom. A view of the transition state showing displacement vectors as well as the dipole unit derivative displacement vector is given in the Supporting Information.

(11) The conversion of **II** into **III-S** was also computed to see whether an interconversion can take place between the P- and C α -protonated forms. This transformation involves a transition that lies +36.3 kcal/mol (B3PW91, 6-311++G**//B3PW91 6-31G*) above **II** and is therefore not conceivable under the experimental conditions used (see Supporting Information).

$J = 25.6$ Hz, $J = 5.1$ Hz, CH, CH_{β} -protonated bond phosphole), 104.4 (d, $J = 66.3$ Hz, C, $\text{C}_{\text{xantheneP}}$), 123.8 (dd, $J = 38.4$ Hz, $J = 4.9$ Hz, C, $\text{C}_{\text{xantheneP}^+}$), 126.8 (d, $J = 14.8$ Hz, CH), 127.8 (d, $J = 14.6$ Hz, CH, $\text{CH}_{\text{phenyl}}$), 128.1 (d, $J = 7.2$ Hz, CH, $\text{CH}_{\text{phenyl}}$), 128.3 (s, C), 128.5 (s, CH), 128.6 (d, $J = 1.8$ Hz, CH), 128.7 (d, $J = 1.8$ Hz, CH), 128.97 (dd, $J = 9.8$ Hz, $J = 2.8$ Hz, CH, C_{β} -protonated phosphole), 129.06 (s, CH), 129.99 (br s, CH), 130.31 (s, CH), 130.41 (d, $J = 3.0$ Hz, CH), 130.5 (s, CH), 130.8 (s, CH), 131.1 (s, CH), 131.3 (s, CH), 131.6 (m, C), 132.1 (d, $J = 7.2$ Hz, CH), 132.2 (d, $J = 7.0$ Hz, CH), 132.9 (d, $J = 11.7$ Hz, C), 133.3 (s, C, $\text{C}_{\text{xanthene}}$), 136.0 (d, $J = 3.0$ Hz, CH), 136.2 (d, $J = 6.9$ Hz, C, $\text{C}_{\text{ipso-phenyl}}$), 136.66 (dd, $J = 35.0$ Hz, $J = 5.2$ Hz, C), 136.72 (s, C), 137.7 (d, $J = 45.8$ Hz, CH), 143.9 (d, $J = 21.7$ Hz, CH), 144.4 (d, $J = 21.2$ Hz, CH), 145.4 (dd, $J = 20.3$ Hz, $J = 6.9$ Hz, C), 150.5 (dd, $J = 18.1$ Hz, $J = 14.3$ Hz, C), 154.5 (d, $J = 3.7$ Hz, C), 156.1 (d, $J = 3.0$ Hz, C). Anal. Calcd for $\text{C}_{47}\text{H}_{37}\text{BF}_4\text{OP}_2$: C, 73.64; H, 4.87. Found: C, 73.51; H, 4.88.

Computational Details. Calculations were realized using the Gaussian 03W set of programs¹² within the DFT framework. The B3PW91 functional^{13,14} was employed in combination with

the 6-31G* basis set for geometry optimizations (for all atoms). Minima were characterized by frequency calculations. The proton affinity (PA) is the negative of the enthalpy change of the reaction, where B and BH^+ denote the base and its conjugate acid. The following equation was used to calculate the absolute proton affinity,¹⁵ where ΔE_{el} represents the difference in electronic energies between the neutral and protonated forms at 0 K. ΔZPE corresponds to the difference in zero-point energies, whereas the last term, $5/2RT$, describes the thermodynamic temperature correction. The absolute proton affinities were calculated at B3LYP/6-311++G(d,p)//HF/6-31G(d,p) and B3PW91/6-311++G(d,p)//B3PW91/6-31G(d,p) level.



$$\text{PA} = -\Delta H = \Delta E_{\text{el}} + \text{ZPE} + \frac{5}{2}RT$$

Acknowledgment. The authors thank the CNRS and the Ecole Polytechnique for financial support of this work, and the IDRIS for the allowance of computer time (Project No. 090616).

Supporting Information Available: Experimental procedures; ^1H and ^{13}C NMR data of compound **2**, ORTEP plot of compound **2**, table of parameters for X-ray crystal structure of **2**, Cartesian coordinates of theoretical structures, three lower frequencies and energies, cif file. This material is available free of charge via the Internet at <http://pubs.acs.org>.

(12) Frisch, M. J.; Trucks, G. W.; Schlegel, H. B.; Scuseria, G. E.; Robb, M. A.; Cheeseman, J. R.; Montgomery, J. A., Jr.; Vreven, T.; Kudin, K. N.; Burant, J. C.; Millam, J. M.; Iyengar, S. S.; Tomasi, J.; Barone, V.; Mennucci, B.; Cossi, M.; Scalmani, G.; Rega, N.; Petersson, G. A.; Nakatsuji, H.; Hada, M.; Ehara, M.; Toyota, K.; Fukuda, R.; Hasegawa, J.; Ishida, M.; Nakajima, T.; Honda, Y.; Kitao, O.; Nakai, H.; Klene, M.; Li, X.; Knox, J. E.; Hratchian, H. P.; Cross, J. B.; Bakken, V.; Adamo, C.; Jaramillo, J.; Gomperts, R.; Stratmann, R. E.; Yazyev, O.; Austin, A. J.; Cammi, R.; Pomelli, C.; Ochterski, J. W.; Ayala, P. Y.; Morokuma, K.; Voth, G. A.; Salvador, P.; Dannenberg, J. J.; Zakrzewski, V. G.; Dapprich, S.; Daniels, A. D.; Strain, M. C.; Farkas, O.; Malick, D. K.; Rabuck, A. D.; Raghavachari, K.; Foresman, J. B.; Ortiz, J. V.; Cui, Q.; Baboul, A. G.; Clifford, S.; Cioslowski, J.; Stefanov, B. B.; Liu, G.; Liashenko, A.; Piskorz, P.; Komaromi, I.; Martin, R. L.; Fox, D. J.; Keith, T.; Al-Laham, M. A.; Peng, C. Y.; Nanayakkara, A.; Challacombe, M.; Gill, P. M. W.; Johnson, B.; Chen, W.; Wong, M. W.; Gonzalez, C.; Pople, J. A. *Gaussian 03*, revision C.02; Gaussian, Inc.: Wallingford, CT, 2004.

(13) Becke, A. D. *J. Chem. Phys.* **1993**, *98*, 5648–5652.

(14) Perdew, J. P.; Wang, Y. *Phys. Rev. B* **1992**, *45*, 13244–13249.

(15) (a) Ann, M. S.; Igor, A. T.; Christopher, J. M. *Theor. Chim. Acta* **1995**, *92*, 83. (b) Zvonimir, B. M.; Borislav, K.; Damir, K. *J. Phys. Chem. A* **1997**, *101*, 7446. (c) Yevgeniy, P.; Leonid, G.; Jerzy, L. *J. Phys. Chem. A* **2000**, *104*, 7346.